

(Blood has a  $T_1$  of 0.4 second in vivo or in vitro with an accuracy of measurement of approximately 0.03 second.) When the bolus arrives at the second coil a dip in the NMR resonance curve is observed in the oscilloscope. By use of a storage oscilloscope or a signal averaging system, the time scale for observation of the polarization reversal and the arrival of the bolus is defined exactly in time.

The arrival of the bolus is reproduced in Fig. 3 as the oscilloscope pattern. The dip in the signal shows when the bolus of fluid arrives at the detection coil. In order to obtain better signal-to-noise ratios, the detected signal is observed every 1/120 of a second and averaged by a signal-averaging system to nullify the random noise. In Fig. 3 we see the envelope of the NMR signals detected by the marginal oscillator detector and averaged over 256 sweeps (each sweep taking 1 second). Measurements of 120 NMR signals per second averaged for 4.25 minutes give the envelope shown in Fig. 3, which shows a venous blood flow velocity of 3.85 cm/sec.

The flow velocity is determined as follows: The inverting pulse is recorded as the start of the scope sweep. The scope face is calibrated at 0.1 sec/cm, and the center of the NMR signal dip is taken as the time ( $t$ ) required for the bolus to reach the center of the NMR receiving coil. Since the distance ( $L$ ) between coils is known, the mean flow velocity is simply  $L/t$ . The measurement shown in Fig. 3 indicates a velocity of blood flow in the median forearm vein of one of us (O.C.M.) of 3.85 cm/sec. We could observe flow measurement times fractionally longer than  $T_1$  because more than one-third of the bolus remains "tagged" for a time longer than  $T_1$ .

As a comparison, flow measurements were also carried out in water and in water solutions of paramagnetic salts. The solutions could be adjusted to have a relaxation time of 0.4 second so as to simulate blood. Using the same instrumental setup as that for the blood flow measurements, we carried out measurements of water flow in a plastic tube. One of the authors previously used this same type of system to measure fuel flow (5).

In the course of these experiments, measurements of the relaxation time ( $T_1$ ) of human blood in vivo as well as in vitro were carried out. Fresh blood was drawn from one of us (O.C.M.) for the in vitro measurement and an anticoagulating agent was added. The effect

of the anticoagulant on relaxation measurements was measured separately, and the anticoagulant was found to have no effect on  $T_1$ . The blood sample in vitro had a  $T_1$  of  $0.4 \pm 0.03$  second. The in vivo measurement gave the same  $T_1$ , in agreement with our earlier measurement on mice (1), and experimenters in the U.S.S.R. (6) have found that dog blood also has a  $T_1$  of 0.4 second.

O. C. MORSE

J. R. SINGER

Cory Hall, University of  
California, Berkeley 94720

#### References and Notes

1. J. R. Singer, *Science* **130**, 1652 (1959).
2. ———, *J. Appl. Phys.* **31**, 125 (1960); *Inst. Radio Eng. Trans. Med. Electron.* **ME-7**, 23 (1960).
3. F. Bloch, *Phys. Rev.* **70**, 474 (1946).
4. N. Bloembergen, E. M. Purcell, R. V. Pound, *ibid.* **73**, 679 (1948).
5. Nuclear magnetic resonance measurements of jet fuel were successfully carried out by J.R.S. on NASA contract No. NAS8-1581.
6. A. Zhernovoi and G. Latyshev, *Nuclear Magnetic Resonance in a Flowing Liquid* (Consultants Bureau, New York, 1965), p. 71.
7. We thank Prof. I. Fatt for the use of part of the equipment, T. Grover for suggestions, and J. Zeevi, Martha Singer, and others who volunteered to be subjects for blood flow measurements.

3 June 1970; revised 27 July 1970

## Bimodal Sedimenting Zones Due to Ligand-Mediated Interactions

**Abstract.** *Ligand-mediated association-dissociation reactions can give rise to band sedimentation patterns showing bimodal bands despite instantaneous establishment of equilibrium. Weaker interactions result in unimodal bands whose sedimentation coefficients decrease with time of sedimentation and in characteristic patterns of total ligand. The implications of these results for fundamental investigations of protein interactions and for conventional analytical applications of zone sedimentation and molecular sieve chromatography are considered.*

Macromolecular interactions mediated by small molecules are important in current thought concerning biological control mechanisms. Binding of ligand molecules to sites on a protein may affect a change in macromolecular conformation or state of aggregation, thereby modulating the biological activity of the large molecule. Of particular interest in the present context are ligand-mediated association-dissociation reactions, examples of which include the facilitated association of carbamyl phosphate synthetase by positive allosteric effectors such as inosine monophosphate or ornithine (1) and the dissociation of lamprey hemoglobin into subunits upon binding oxygen (2). Both of these reversible reactions were detected and studied by the method of sedimentation velocity—zone sedimentation through a preformed density gradient in the first instance and moving-boundary analytical sedimentation in the second. For some time we have been developing the theory of sedimentation of ligand-mediated interactions of this sort (3; 4, chapters 4 and 5), since such calculations provide one with the understanding required for quantitative, indeed, sometimes even qualitative, interpretation of their sedimentation patterns.

Consider, for example, the reversible reaction



in which a macromolecule M associates into a polymer containing  $m$  monomeric units ( $m$ -mer), with the mediation

of a small molecule or ion X, of which a fixed number  $n$  are bound into the complex. The set of conservation equations for sedimentation in a sector-shaped ultracentrifuge cell takes the form

$$\frac{\partial(C_1 + mC_2)}{\partial t} = \frac{1}{r} \frac{\partial}{\partial r} \left[ (D_1 \frac{\partial C_1}{\partial r} - C_1 s_1 w^2 r) r + m (D_2 \frac{\partial C_2}{\partial r} - C_2 s_2 w^2 r) r \right] \quad (1)$$

$$\frac{\partial(nC_2 + C_3)}{\partial t} = \frac{1}{r} \frac{\partial}{\partial r} \left[ n(D_2 \frac{\partial C_2}{\partial r} - C_2 s_2 w^2 r) r + (D_3 \frac{\partial C_3}{\partial r} - C_3 s_3 w^2 r) r \right]$$

In these equations  $C$  designates molar concentration;  $D$ , diffusion coefficient;  $s$ , sedimentation coefficient;  $w$ , angular rotation;  $r$ , radial distance; and  $t$ , time. The subscripts 1, 2, and 3 designate M,  $M_mX_n$ , and X, respectively. The calculations have been made for rates of reaction very much larger than the rates of diffusion and sedimentation so that local equilibrium attains at every instant. In this limit

$$C_2 = KC_1^m C_3^n$$

where  $K$  is the equilibrium constant of the reaction. A rapid and accurate calculation has been formulated for the numerical solution of these equations (4, chapter 5). The computer code (5) is written so as to be applicable not only

to ligand-mediated macromolecular association but also to interactions of the type

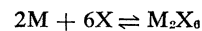


in which the binding of small ligand to macromonomer causes dissociation of an  $m$ -mer into its hydrodynamically identical subunits. Moreover, appropriate choice of initial and boundary conditions permits computation of either moving-boundary or band sedimentation patterns. Theoretical sedimentation patterns (Figs. 1–6) are displayed either as gradient curves, which are plots of

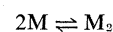
$\partial(C_1 + mC_2)/\partial r$  as a function of  $r$ , or as integral curves, that is, plots of  $C_1 + mC_2$  as a function of  $r$ . The subscripts 1 and 2 refer to monomer and  $m$ -mer for both ligand-mediated association and ligand-mediated dissociation reactions. Initial equilibrium concentrations of macromonomer,  $m$ -mer, and unbound ligand are designated as  $C_{10}$ ,  $C_{20}$ , and  $C_{30}$ , respectively.

Previous calculations of moving-boundary sedimentation patterns for ligand-mediated interacting systems are discussed in detail elsewhere (4, chapter 4), but a brief comment on their impli-

cations for analytical sedimentation is warranted here. The theoretical patterns presented in Fig. 1 are for the reaction



in which the dimerization of a macromolecule is mediated by the binding of six ligand molecules into the complex. Such an interaction can give rise to a well-resolved bimodal reaction boundary (Fig. 1B) despite the instantaneous establishment of equilibrium. Resolution of the two peaks depends upon the production and maintenance of concentration gradients of unbound ligand along the centrifuge cell by reequilibration during differential transport of macromonomer and dimer; and the higher the cooperativeness of the interaction (that is, the larger  $n$ ), the better the resolution. The peaks correspond to different equilibrium mixtures and not simply to monomer and dimer. In general, their relative areas do not faithfully reflect the initial equilibrium composition and are sensitive to rotor speed. Nor are their rates of sedimentation the same as those of the monomer and dimer. Under some conditions the sedimentation coefficient of the slow peak is greater than that of the monomer since the mixture represented by the slow peak contains dimer, whereas the sedimentation coefficient of the fast peak is always less than that of the dimer since the corresponding mixture contains monomer. Such behavior is in contradistinction to that predicted by the Gilbert theory (6) and observed experimentally (7) for a simple dimerization of the type



Systems of this sort always give sedimentation patterns showing a single peak with a weight-average sedimentation coefficient when reequilibration is rapid. Of course, at sufficiently high ligand concentration (or low centrifugal field) ligand-mediated dimerization will also give patterns that show a single peak. In the limit where for any reason the concentration of unbound ligand along the centrifuge cell is not significantly perturbed by the reaction during differential sedimentation of the macromolecular species, the system effectively approaches the case of simple dimerization considered by Gilbert.

Recently, Morimoto *et al.* (8) have found that (i) the reversible dimerization of New England lobster hemocyanin that occurs when the pH is lowered from above 9.6 to below 9.2 in the

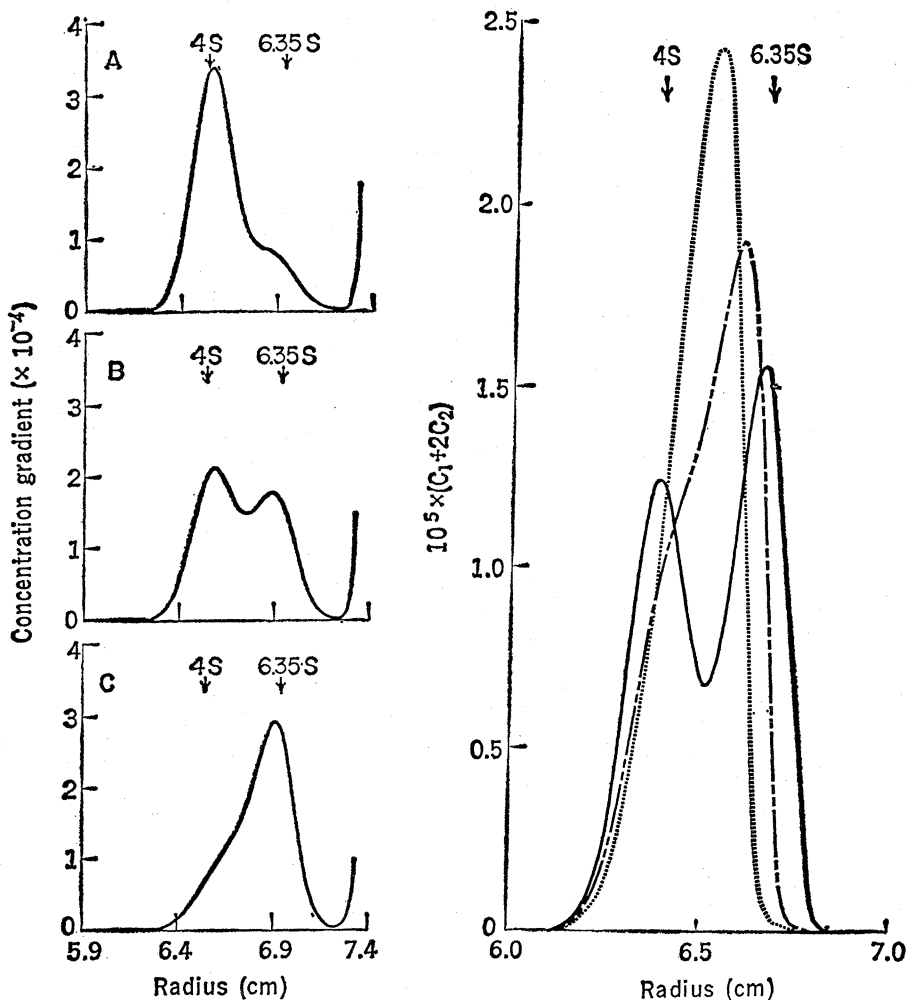


Fig. 1 (left). Theoretical moving-boundary sedimentation patterns for the ligand-mediated dimerization reaction,  $2M + 6X \rightleftharpoons M_2X_6$ . Dependence of boundary shape upon percentage of dimerization,  $K = 4.57 \times 10^{20} M^{-7}$ : (A) 25 percent dimerization,  $C_{30} = 3.89 \times 10^{-5} M$ ; (B) 50 percent,  $5 \times 10^{-5} M$ ; (C) 75 percent,  $6.74 \times 10^{-5} M$ . The following values of macromolecular concentrations and parameters were chosen (4) to approximate the sedimentation of a protein of molecular weight 60,000:  $C_{10} + 2C_{20} = 14 \times 10^{-5} M$ ,  $s_1 = 4S$ ,  $s_2 = 6.35S$ ,  $D_1 = 6 \times 10^{-7} \text{ cm}^2 \text{ sec}^{-1}$ ,  $D_2 = 4.76 \times 10^{-7} \text{ cm}^2 \text{ sec}^{-1}$ . For the small molecule:  $s_3 = 0.15S$ ,  $D_3 = 10^{-5} \text{ cm}^2 \text{ sec}^{-1}$ . Rotor speed, 60,000 rev/min. Time of sedimentation, 6431 seconds. [Courtesy of Academic Press, Inc.] Fig. 2 (right). Theoretical band sedimentation patterns for the ligand-mediated dimerization reaction,  $2M + 6X \rightleftharpoons M_2X_6$ : 50 percent dimerization; ———,  $C_{30} = 10^{-5} M$ ; — — — —,  $10^{-5} M$ ; ·····,  $5 \times 10^{-5} M$ . Unbound ligand initially distributed uniformly throughout the centrifuge cell. Time of sedimentation, 4740 seconds at 60,000 rev/min;  $s_3 = 0.15S$ ; other parameters as in Fig. 1.

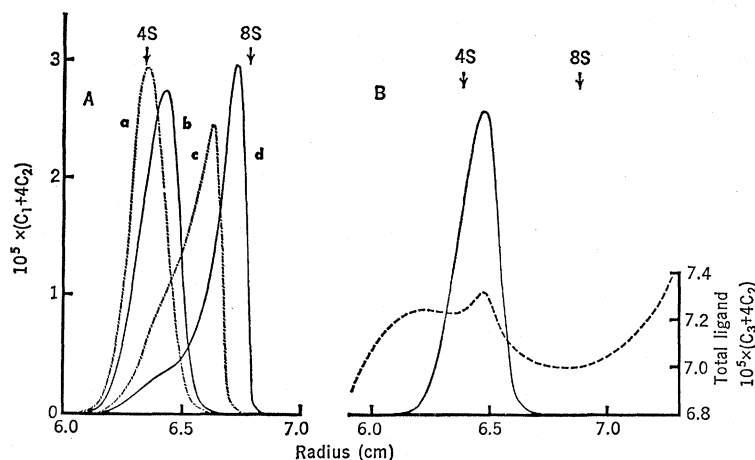


Fig. 3 (left). Theoretical band sedimentation patterns for the ligand-mediated tetramerization,  $4M + 4X \rightleftharpoons M_4X_4$ . (A) Patterns *a* and *b* computed for 50 percent tetramer,  $C_{30} = 7 \times 10^{-5}M$ ; patterns *c* and *d* for 90 percent tetramer,  $C_{30} = 1.4 \times 10^{-5}M$ ; patterns *a* and *c* for unbound ligand initially present only in the starting band; patterns *b* and *d* for unbound ligand initially distributed uniformly throughout the centrifuge cell. (B) Comparison of macromolecule pattern, ———, with total ligand pattern, ———, for 50 percent tetramer;  $C_{30} = 7 \times 10^{-5}M$  throughout the centrifuge cell.  $C_{10} + 4C_{20} = 14 \times 10^{-5}M$ ,  $s_1 = 4S$ ,  $s_2 = 8S$ ,  $s_3 = 0.15S$ ;  $D_1 = 6 \times 10^{-7} \text{ cm}^2 \text{ sec}^{-1}$ ,  $D_2 = 3.8 \times 10^{-7} \text{ cm}^2 \text{ sec}^{-1}$ , and  $D_3 = 10^{-6} \text{ cm}^2 \text{ sec}^{-1}$ ; 4250 seconds at 60,000 rev/min.

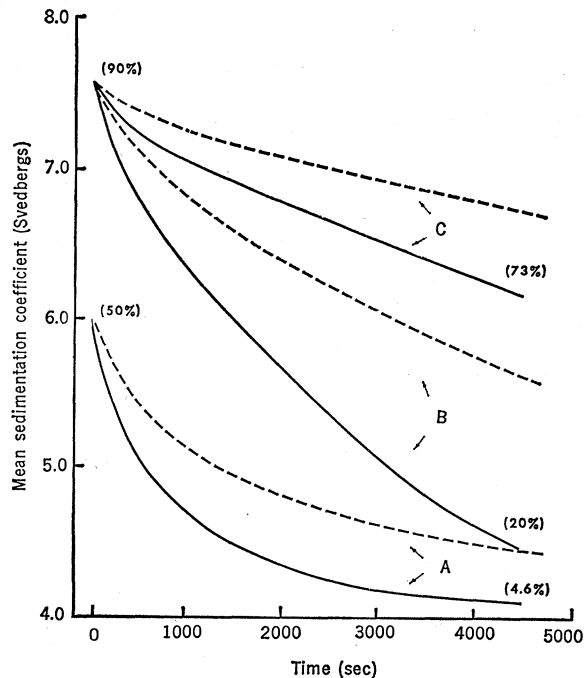


Fig. 4 (right). Dependence of mean sedimentation coefficient upon time of sedimentation: ———, instantaneous sedimentation coefficient computed from first moments at about 470-second intervals; ———, sedimentation coefficient computed from the first moment of the band at a given time and the first moment of the initial band. Curves *A* were computed for those conditions that gave pattern *b* in Fig. 3, that is, for 50 percent tetramer and  $C_{30} = 7 \times 10^{-5}M$  throughout the cell; curves *B* and *C*, for patterns *c* and *d* (Fig. 3), that is, 90 percent tetramer and  $C_{30} = 1.4 \times 10^{-5}M$  in the initial band only or throughout the cell, respectively. The initial percentage of tetramer and the percentage at the position of the maximum of the band after 4720 seconds are shown in parentheses.

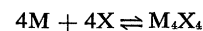
presence of  $\text{Ca}^{2+}$  is mediated by the binding of four to six  $\text{Ca}^{2+}$  ions and two to four  $\text{H}^+$  ions; (ii) both the forward and the reverse reactions are very rapid; and (iii) the sedimentation patterns in this *pH* range show two peaks, as predicted above, for such an interaction. Thus, this experiment demonstrates once again that the sedimentation patterns of interacting systems must be interpreted with caution, and that proof for inherent heterogeneity ultimately depends upon the isolation of the various components.

Our calculations have now been extended to include band sedimentation, and the results are in certain respects analogous to those described above for moving-boundary sedimentation. A particularly pregnant result is that ligand-mediated associating-dissociating systems can give bimodal reaction bands even though reequilibration is rapid. The band patterns displayed in Fig. 2 for 50 percent dimerization mediated by the binding of six ligand molecules into the complex illustrate the way in which resolution depends upon ligand concentration. For an appropriate choice of ligand concentration the band is well resolved into two intense peaks. The sedimentation coefficient of the

slow peak is the same as for the macromonomer, whereas that of the fast peak is only slightly less than that for the dimer; but the amount of material in each peak does not correspond to the amount of monomer and dimer in the initial equilibrium mixture. Increasing the initial ligand concentration while holding the percentage of dimerization constant results in progressive coalescence of the two peaks with concomitant drift in their sedimentation coefficients toward a value close to the weight-average sedimentation coefficient until resolution disappears entirely at the highest concentration. This result can be understood as follows: The weaker the interaction and thus the higher the concentration of unbound ligand for a given percentage of dimerization, the more difficult it becomes to produce the concentration gradients of free ligand upon which resolution depends. These calculations are for unbound ligand initially distributed uniformly throughout the centrifuge cell, but a bimodal band of virtually the same shape as that shown in Fig. 2 was obtained when the computation was for the same concentration of unbound ligand initially present only in the starting band. This too is readily understood: For a strong inter-

action there is so much more bound than free ligand that a small amount of dissociation of the complex is sufficient to maintain the equilibrium concentration of free ligand as the band moves down the cell. As one might expect, there is a relationship between the conditions for resolution and the cooperativeness of the interaction. Thus, a well-resolved band was obtained for  $n = 30$  at a concentration of unbound ligand an order of magnitude greater than for  $n = 6$ , whether or not ligand was distributed throughout the cell initially.

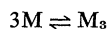
The unimodal band obtained at the highest ligand concentration (Fig. 2) is somewhat skewed centripetally, and its mean sedimentation coefficient decreases about 10 percent during the course of sedimentation as a result of some dissociation of the dimer within the spreading zone. This behavior assumes major proportions in the case of ligand-mediated tetramerization,



Consider, for example, 50 percent tetramerization, at equal constituent concentrations of ligand and macromolecule (Figs. 3A and 4A). The mean sedimentation coefficient of the predicted unimodal band decreases rapidly and con-

tinuously from the weight-average value to a value approaching that of the macromonomer as the band migrates down the centrifuge cell, that is, as the band spreads as a result of differential transport of  $M$  and  $M_4X_4$  and diffusion. In fact, for all practical purposes it can be said that the rate of sedimentation of the system is essentially the same as that of the monomer. This is certainly so when ligand is initially present only in the starting zone and approximately so when ligand is initially distributed throughout the cell. Such behavior reflects the strong concentration dependence of tetramerization; as the macromolecular concentration within the spreading band decreases, the tetramer dissociates by mass-action into monomer with a slower rate of sedimentation. Even for much stronger interaction (90 percent tetramerization at equal constituent concentrations of ligand and macromolecule) the theory predicts a band

shape indicative of dissociation of the tetramer (Fig. 3A) and a mean sedimentation coefficient that decreases markedly with time of sedimentation (Fig. 4, B and C). The shape of the band for the case in which ligand is initially distributed throughout the cell approaches that computed by Bethune and Kegeles (9) for the simple trimerization reaction,



For conditions such that dissociation plays a decisive role in determining sedimentation behavior as, for example, in the aforementioned case of 50 percent dimerization, one might expect a distinctive distribution of ligand through the cell. As illustrated in Fig. 3B, this is indeed the case. Whereas the band of macromolecule is unimodal, the distribution of total ligand is bimodal, provided that free ligand is initially distributed uniformly along the cell. The

bimodal distribution of total ligand is generated as follows: As the tetramer dissociates it releases ligand, which remains behind the advancing band of macromolecule. The sum of the broad band of released ligand, the relatively narrow band of ligand bound to the remaining tetramer, and the distorted background of unbound ligand is bimodal. An observation of this sort together with a nonlinear dependence of the logarithm of the mean position of a unimodal macromolecular band upon time evidently constitutes unambiguous evidence for ligand-mediated association. Finally, ligand-mediated tetramerization cannot give a bimodal band of macromolecule except for the trivial situation in which the interaction is so very strong that for all practical purposes macromonomer and tetramer sediment independently; for example, 90 percent tetramer,  $C_{30} = 10^{-8}M$  throughout the cell. For nontrivial con-

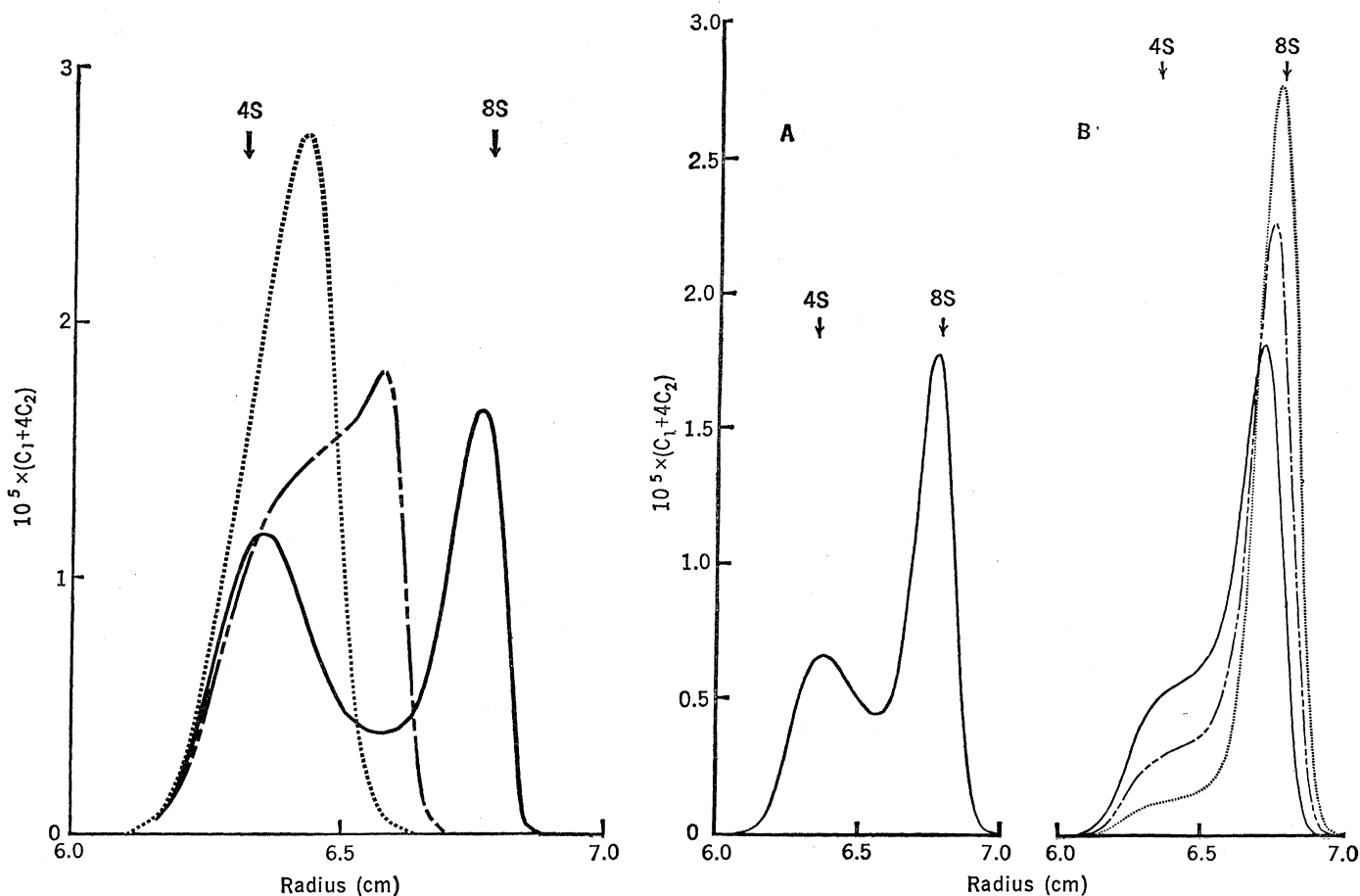
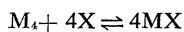


Fig. 5 (left). Theoretical band sedimentation patterns for the ligand-mediated dissociation reaction,  $M_4 + 4X \rightleftharpoons 4MX$ : 50 percent dissociation; ———,  $C_{30} = 10^{-8}M$ ; - - - - - ,  $7 \times 10^{-8}M$ ; ······,  $7 \times 10^{-8}M$ . Unbound ligand initially distributed uniformly throughout the centrifuge cell.  $C_{10} + 4C_{20}$  and other parameters as in Fig. 3. Fig. 6 (right). Theoretical band sedimentation patterns for the ligand-mediated dissociation reaction,  $M_4 + 4X \rightleftharpoons 4MX$ . (A) 50 percent dissociation,  $C_{30} = 7 \times 10^{-8}M$ ; (B) ———, 75 percent dissociation,  $C_{30} = 6.24 \times 10^{-8}M$ ; - - - - - , 50 percent,  $3.5 \times 10^{-8}M$ ; ······, 25 percent,  $1.5813 \times 10^{-8}M$ . Unbound ligand initially present only in the starting band.  $C_{10} + 4C_{20}$  and other parameters as in Fig. 3.

ditions (for example, 50 percent tetramer,  $C_{30} = 10^{-6}M$ ) the band shows at most a leading peak with a broad, intense shoulder, the sedimentation coefficient of the peak being considerably less than that of the tetramer.

A different behavior is shown by the ligand-mediated dissociation reaction



Theoretical band patterns for 50 percent dissociation with unbound ligand initially distributed throughout the cell are displayed in Fig. 5. In contrast to ligand-mediated tetramerization the pattern computed for  $C_{30} = 10^{-6}M$  is a well-resolved, bimodal reaction band. This contrasting behavior may be explained as follows: The two factors that govern the equilibrium—protein concentration and total ligand concentration—both diminish as the zone spreads. The decrease in total ligand concentration produces the asymmetry between mediated association and mediated dissociation, for in the one case ligand promotes association, and in the other ligand promotes dissociation. As the ligand concentration is increased with the percentage of dissociation held constant (Fig. 5), that is, as the interaction becomes weaker, it becomes progressively more difficult to perturb the concentration of unbound ligand significantly during differential sedimentation of the macromolecular species, and dissociation of the tetramer as a result of dilution of the macromolecule within the spreading band becomes the dominant factor in determining sedimentation behavior. Thus, at the highest ligand concentration the rate of sedimentation of the macromolecule approximates that of the monomer. In fact, the unimodal band is indistinguishable from that shown in Fig. 3B for 50 percent ligand-mediated tetramerization at the same ligand concentration; and the dependence of the mean sedimentation coefficient of the unimodal band upon time is also identical. There is one important difference, however: the total ligand pattern shows only a single peak whose sedimentation coefficient is the same as that of the macromolecule band. This difference is one way of distinguishing the two interactions in practice. Another way would be to determine the dependence of the extrapolated mean sedimentation coefficient upon ligand concentration. For macromolecular association the sedimentation coefficient will increase with increasing ligand con-

centration, whereas for dissociation it will decrease. Finally, when the ligand is initially present only in the starting band, the theoretical pattern (Fig. 6) exhibits bimodal bands or bands showing a major fast peak and a broad, often intense, centripetal shoulder over a wide range of parameters (25 to 90 percent dissociation;  $C_{30} = 7 \times 10^{-6}M$  to  $7 \times 10^{-4}M$ ;  $C_{10} + 4C_{20} = 6 \times 10^{-5}M$  to  $14 \times 10^{-5}M$ ). The material represented by the fast peak generally migrates with a sedimentation coefficient close to that of the tetramer and the material represented by the slow peak or shoulder, with a sedimentation coefficient close to that of the monomer; but the distribution of material between the two peaks does not conform to the initial equilibrium composition. The amount corresponding to the slow peak, while increasing with increasing fraction dissociated, is in all cases considerably less than the amount reckoned from the initial equilibrium concentration of monomer.

Although the theory described above is for a sector-shaped cell and instantaneously varying sedimentation velocities of the several species, the results can be applied to rectilinear situations and constant velocities with only quantitative reservations. Accordingly, the results have important implications for the many conventional analytical applications of zone velocity sedimentation through a preformed density gradient in the preparative ultracentrifuge and molecular sieve chromatography on Sephadex or other gel-permeation supports. Thus, for example, ligand-mediated interactions can give bimodal reaction zones.

Possible complications of this sort will become evident, however, when the fractions themselves are examined under the same conditions as those used in the original separation to see if they run true. Careful note should also be taken of the difference between the macromolecule and total ligand patterns presented in Fig. 3B, since it is not uncommon in practice to follow zone sedimentation by analysis of fractions for specific ligand (10). This is often the only method available for detecting a given protein in a partially purified extract; but it must be borne in mind that a bimodal distribution of ligand need not necessarily indicate inherent heterogeneity. Nor would it seem to be unique for interactions characterized by macromolecular association. Con-

ceivably, pressure-sensitive ligand binding without a change in state of aggregation or frictional coefficient would give a similar result if pressure favored the dissociation of the complex(es). In that event, however, the sedimentation coefficient of the protein zone would not decrease with time of sedimentation. It is generally not practical to follow the time course of development of zone sedimentation patterns in the preparative instrument. Consequently, the decrease in sedimentation coefficient of the unimodal zone predicted for weak interactions would go undetected. If circumstance attending an unusual sedimentation behavior of a unimodal zone (for example, increasing sedimentation coefficient with increasing protein concentration in the known presence of ligand) indicates ligand-mediated association-dissociation, the system should be examined by band sedimentation, and the instantaneous sedimentation coefficient should be extrapolated to zero time in order to characterize the interaction quantitatively. In this light, the facilitated association of carbamyl phosphate synthetase by positive allosteric effectors (1) bears reinvestigation.

JOHN R. CANN

Department of Biophysics,  
University of Colorado Medical  
Center, Denver 80220

WALTER B. GOAD

University of California Los  
Alamos Scientific Laboratory,  
Los Alamos, New Mexico 87544

#### References and Notes

1. P. M. Anderson and S. V. Marvin, *Biochemistry* **9**, 171 (1970).
2. R. W. Briehl, *J. Biol. Chem.* **238**, 2361 (1963).
3. J. R. Cann and W. B. Goad, *Advan. Enzymol.* **30**, 139 (1968); W. B. Goad and J. R. Cann, *Ann. N.Y. Acad. Sci.* **164**, 172 (1969).
4. J. R. Cann and W. B. Goad, *Interacting Macromolecules: The Theory and Practice of Their Electrophoresis, Ultracentrifugation, and Chromatography* (Academic Press, New York, 1970).
5. A copy of the computer code (4, chapter 5) will be supplied by W.B.G. upon request.
6. G. A. Gilbert, *Discuss. Faraday Soc.* **20**, 68 (1955); *Proc. Roy. Soc. London Ser. A Math. Phys. Sci.* **250**, 377 (1959).
7. E. O. Field and J. R. P. O'Brien, *Biochem. J.* **60**, 656 (1955); E. O. Field and A. G. Ogston, *ibid.*, p. 661.
8. K. Morimoto, M. Tai, G. Kegeles, Abstracts of Papers, Joint Chemical Institute of Canada-American Chemical Society Conference, Toronto, 24-29 May 1970; Colloid 11.
9. J. L. Bethune and G. Kegeles, *J. Phys. Chem.* **65**, 433 (1961).
10. W. Gilbert and B. Müller-Hill, *Proc. Nat. Acad. Sci. U.S.A.* **56**, 1891 (1966).
11. Supported in part by NIH research grant 5 R01 AI01482. Dr. Goad's work was done under the auspices of the U.S. Atomic Energy Commission, Contribution No. 414 from the Department of Biophysics, Florence R. Sabin Laboratories, University of Colorado Medical Center, Denver 80220.

10 June 1970; revised 24 July 1970